

# The Strategy of Energy Saving for Smart Shipping

Heiu-Jou Shaw<sup>1</sup>, Fu-Ming Tzu<sup>2,\*</sup>

<sup>1</sup>Department of System and Naval Mechatronic Engineering, National Cheng Kung University, Tainan, Taiwan

<sup>2</sup>Department of Marine Engineering, National Kaohsiung University of Science and Technology, Kaohsiung, Taiwan

Received 13 March 2019; received in revised form 22 April 2019; accepted 25 May 2019

## Abstract

This paper presents a real record and analysis to reduce carbon dioxide (CO<sub>2</sub>) emission and fuel consumption using the energy efficiency operational index (EEOI) for practical ships. With giant commercial tankers constantly launching into the sea, emission increase with the tonnage is unavoidable. More weight means more pollution. In the experiment, big data of Internet of Things (IoT) were collected to analyze the sailing conditions for over six months through global satellite communications while the ship sailed across the ocean. The results showed that deep draft results in a better performance than shallow draft; that is, the ship carries more cargo but consumes less fuel oil, as opposed to the traditional concept. Among the parameters, the draft and cargo mass interacts with the index to identify the fuel consumption at a constant speed; A draft between 11.5 m and 12 m was found to be optimum for this type of container ship. The EEOI is a metric tool to illustrate the variation of fuel consumption and an effective management strategy to reduce the CO<sub>2</sub> emission quantity. Moreover, a constructive model using IoT technology and an energy efficiency management strategy presents an accurate big data basis to guide decision making on the vessel.

**Keywords:** cargo loading, speed over ground, average draft, fuel consumption, energy efficiency operational index (EEOI)

## 1. Introduction

Following the booming shipping market, giant container ships now constantly launch into the sea; thus, greenhouse gas pollution is getting more severe due to the increasing carbon dioxide (CO<sub>2</sub>) emission [1, 2]. Therefore, an effective method to evaluate the emission [3-5] is urgently needed. The energy efficiency operational index (EEOI) [6, 7] is a metric unit that measures the CO<sub>2</sub> emission of a ship and also predicts the consumption of the fuel oil in the vessel. Presently, energy saving is an extremely necessary task on board since the container ship is always on missions across the oceans so that schedules to improve energy saving are hardly made. Furthermore, the International Convention for the Prevention of Pollution from Ships, adopted by the International Maritime Organization (IMO), is the standard guiding the energy efficiency of ships [8]. Moreover, the measurement of the performance indicator refers to ISO19030, which describes the measurement of changes in the hull and propeller parameter for energy efficiency [8].

Recently, big data analysis has become a mainstream statistical method for maritime management for global shipping [9]. Various shipping companies utilize smart shipping to analyze the navigational attitude, loading, nacelle, and sea weather information, and this improves the energy efficiency to enhance sailing safety. In the globalization era, the shipping industry has become a key factor of the economy in a world where over 90% of global trade is seaborne [10]. Moreover, the weight scale of container ships is in megatonnage; thus, in this study, we use current data recorded in a ship to measure the emission

---

\* Corresponding author. E-mail address: fuming88@nkust.edu.tw

Tel.: +886-7-8100888#25245; Fax: +886-7-5716043

pollution. If the shipping industry were a country, its CO<sub>2</sub> emission would be higher than that of Germany [2]. The industry accounts for 3% of the world's CO<sub>2</sub> emission, ranking as the seventh-largest seventh emitter among countries. In 2013, the IMO, aiming at energy saving in ships, enforced regulation for emission control that mandates every shipping company to build a self-project based on the ship energy efficiency management plan (SEEMP). However, the SEEMP cannot reflect the real consumption of fuel oil without the EEOI. The EEOI is voluntary behavior to take the measured by own shipping. When a ship sails across the ocean from country to country, especially to an emission control area [11, 12], it follows rather strict regulations; the regulation can help control the pollution and carbon emission quantity.

The paper contributes two aspects to reduce CO<sub>2</sub> emission and save fuel consumption. First, the relationships between power efficiency and speed as well as power efficiency and trim at various drafts are analyzed. Second, an EEOI-based strategy for ship energy management is presented. The measured parameters include engine power, trim, draft, fuel consumption, cargo mass, and weather condition.

## 2. Systematic Architecture

This work is focused on the evaluation of energy saving for ships using the EEOI metric. We selected a practical container ship to install a digital device that functions based on the Internet of Things (IoT) technology. The device collects the sailing information and creates a whole communication system between the headquarter (HQ) and ship for energy efficiency by big data analysis (Fig. 1). An EEOI-based energy efficiency strategy can then be suggested for improving efficiency and thus saving energy.

The installed device consists of a vessel data recorder and an alarm monitoring system (AMS). The data are transferred to the HQ by AMOS Software (Spec Tec Group Holding Ltd, Italy) using satellite communication and fed back to the ship [13], using the GlocalMe WiFi all-day network service. The devices are installed in the engine room and bridge, and the sub-server is installed inside the electrical room where the big data of a particular parameter are transferred to the main server. This is a novel forward-looking method to manage energy efficiency through big data analysis, whereby the data model is constructed using EEOI, and valuable information is provided to decision makers for smart shipping.

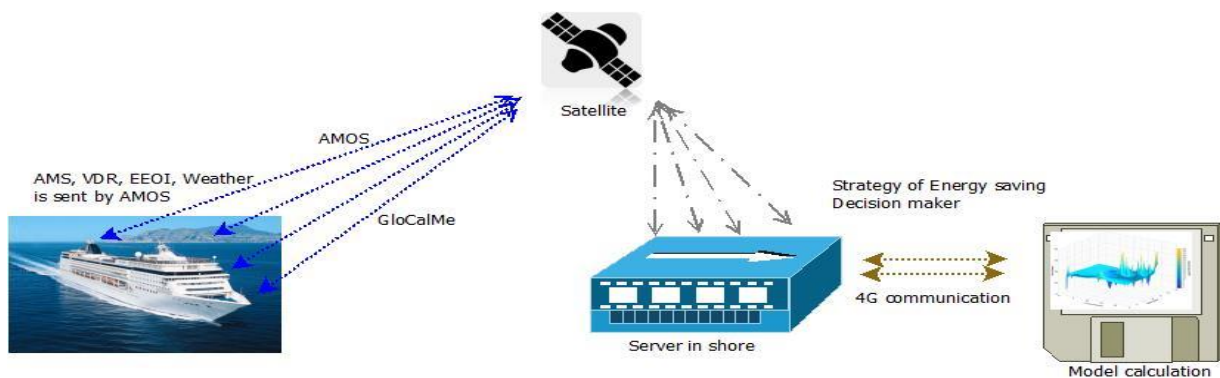


Fig. 1 Communication involving big data using satellite on a practical ship

The ship's big data architecture is divided into three layers. The first layer collects the hardware information of the ship. At this stage, the sensing layer, that is, the installed active sensor, collects information on time from the host (auxiliary machines, and power centers); such information includes navigational information, such as draft, speed, load, and climate condition, and actual operational information. In addition, the fiber optic sensor detects the main shaft speed, and the mass flow meter collects the fuel state. The second layer is the network layer. The information detected by each sensor is collected into the gateway and then enters the router. A wired or wireless network connection is used. When the information packet enters the server, the statistical program automatically begins to connect the satellite communication. The shore-based HQ of the traffic control center and the land data center complete the networking function, and the data are scheduled to be sent to the designated

address. The third layer is the application layer. The big data collection is not only used by a single ship; the statistical program structure data are analyzed by the host computer and the server to connect the data to the same type of ship, allowing the fleet to use the data simultaneously. The construction of this system can maximize the application of energy efficiency of the entire ship, which enhances convenient pipeline operations in maritime science for exploration, supporting the practitioners, and reducing marine accidents.

The evaluation is based on the EEOI metric unit to examine the fuel oil consumption and CO<sub>2</sub> emission per distance (nautical mile) for a period of over six months, from Feb. 8 to Aug. 3, 2018. The evaluated parameters in the experiment include EEOI, cargo mass, fuel consumption, distance, avg. draft, and trim by the fore and stern of a practical ship.

### 3. Data Acquisition

The data were acquired at a steady rate to measure the hull and propeller parameters [14]; the digital device of big data analysis was used in the experiment to acquire information. The digital data were selected to measure the loading of the container ship every five minutes. The data were collected on board for a voyage of six months: 166 days in the sea and 14 days in the port; that is, for roughly 92% of the operation time, the ship was in activity. Data were still collected when the ship was at the harbor. The steering angle frequently varied due to ship operations, such as entering or departing the harbor, and special conditions. Moreover, to fulfill the safety requirements, the speed of the ship was adjusted by the captain, who manipulated the ship to avoid collision during the course. The engine order and rudder order in the interaction often varied for safe navigation. Normally, the “ahead” orders of the ship consist of stop, standby, dead slow ahead, slow ahead, half ahead, full ahead. If the ship needs an astern, then the orders include dead slow astern, slow astern, half astern, and full astern.

The sensor device installed in the ship is very challenging in the task which the marine equipment must maintain at safety operation, and the installed device cannot affect operation. The acquired parameters, which include fuel consumption, loading change, draft, and trim profile, were analyzed through big data analysis. In addition, due to various weather conditions, the sea wave significantly affected speed. The speed over ground (SOG) is the same as the speed displayed on the global position system (GPS). Furthermore, the ship was manipulated by autopilot while sailing in the wide ocean. However, for safety, the steering gear can be released by hand pilot to avoid an accident.

The EEOI is a metric unit to quantify CO<sub>2</sub> emission and a method to evaluate fuel consumption [6, 7]. According to the IMO, the EEOI can be expressed as the product of the CO<sub>2</sub> factor of transfer coefficient and fuel consumption divided by the product of carrier cargo and sailing distance:

$$\text{Average EEOI} = \sum_{1}^{n} \frac{\text{CO}_2 \text{ factor} \times \text{FOC (tonne)}}{\text{cargo mass (tonne)} \times \text{sailed distance (nautical mile)}} \quad (1)$$

Here,  $n$  is the total number of voyage segments over the period. A CO<sub>2</sub> factor of 3.114 (t-CO<sub>2</sub>/t-fuel) was assumed in our experiment, based on the heavy fuel oil at the type of main engine [15]. The FOC means fuel consumption during the voyage every five minutes for over six months. Hence, the numerator represents the CO<sub>2</sub> emission of fuel consumption. Typically, the large two-stroke cycle of marine engine uses the heavy fuel oil to supply the main power. On the other hand, the denominator represents the cargo mass carried during the voyage. A large denominator, i.e., small EEOI, is based on a certain consumption of fuel oil, and it means higher efficiency of the ship. In this study, the EEOI at the ship varied from  $1 \sim 3 \times 10^{-5}$ , depending on the parameters. Thus, we anticipate the measurement method will save fuel oil consumption and reduce the CO<sub>2</sub> emission to support the marine industry.

The main engine (manufactured by MAN B&W), which is a typical diesel engine of the large two-stroke cycle using heavy fuel oil, was installed in the ship. The technical specifications are presented in Table 1.

Table 1 The technical data of the ship in the experiment

Item	Description	Unit
Launch Date	2012	-
Main Engine Type	MAN B&W 12K98MC	-
Main Engine Power	68,640 kW	-
Container Capacity	8200	TEU
Length Over All	333.2	meter
Depth (molded)	24.2	meter
Breath (molded)	42.8	meter
Scantling Draft (molded)/Summer Draft	14.5	meter
Gross Tonnage	90,532	-
Net Tonnage	41,396	Ton
Deadweight Tonnage/D.W.T	103,235	Ton
Main Engine Revolution Per Minute	94	rpm
Service Speed	25	knot

#### 4. Result and Discussion

The experiment was carried out using a practical ship that sailed across the Pacific Ocean to the Atlantic Ocean. First, through satellite communication, the digital device installed on the board timely transferred information to the HQ, and a big data analysis was performed in the ship. The ship's route (Fig. 2) was from Taiwan, Hong Kong, China to the east coast of the USA throughout Panama Canal, back and forth. The ship traveled a total distance of 55,000 nautical miles with four voyages during the period. However, temporary disconnection of satellite communication on the vessel was sometimes unavoidable due to unpredictable bad weather or poor transmission at sea. There was a small broken route during the period, as shown in Fig. 2, to express bad communication in the vessel. However, the temporary disconnection will not affect the experiment since the data can be saved and transferred to the HQ after the communication is restored.

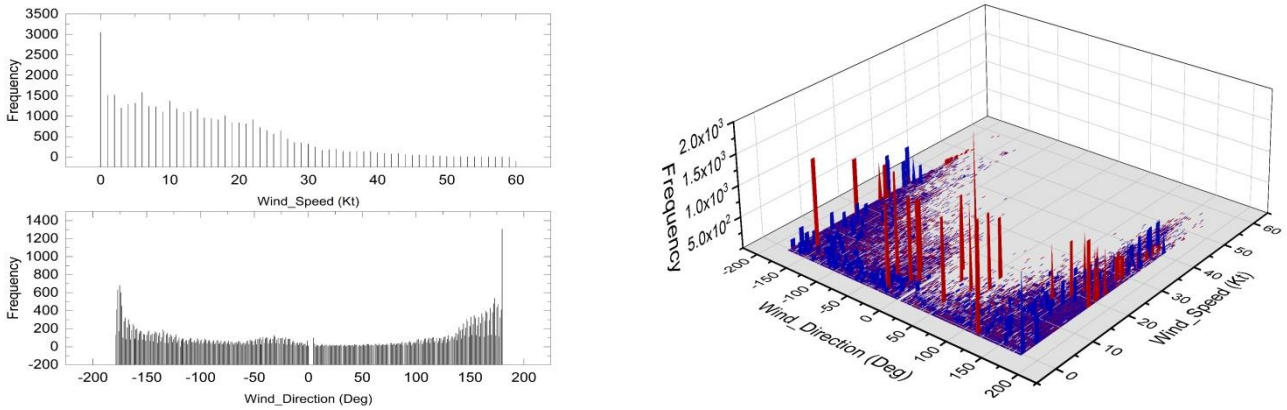


Fig. 2 Electronic chart of 2D route illustrating the trace of the ship

A combined statistical distribution of the relative wind speed and direction is presented in Fig. 3. The upper Fig. 3(a) illustrates the frequency statistics of the relative wind speed at each section; the occurrences from 0 to 60 knots is about 3,000 times at 0 knots, 1,500 times at 10 knots, and 1,000 times at 20 knots, descending sequentially. The lower Fig. 3(a) displays the frequency statistics of the wind direction angle, from  $-180$  degrees to  $+180$  degrees. The wind direction angle is 0 degree at the bow, 0 to  $+180$  degrees on the starboard side, and 0 to  $-180$  degrees on the port side. Compared with the occurrences of wind speed, the wind direction angle appears denser. Except for 180 degrees at 1200 times, the average angle is about 200 times. Therefore, the wind direction angle is denser than the relative wind speed. The Fig. 3(b) shows the combined distribution of the upper and lower Fig. 3(a) diagrams, where blue represents the relative wind direction and red represents the relative wind speed.

Fig. 4 is a distribution of the relative wind direction and relative wind speed for fuel consumption during the ship navigation. The lateral coordinate presents relative wind speeds, and the longitudinal coordinate displays a relative wind direction. When the ship was heading at the 0-degree course, the positive wind direction came from the bow, whereby the bow

is represented by a 0-degree angle. When the ship hull area was larger, the resistance was greater, which was caused by the positive wind direction. In addition, the color bar on the right of Fig. 4 indicates the amount of fuel consumption. The red color indicates large fuel consumption, which sequentially decreases in the downward direction. The blue area presents a small fuel consumption. The wind direction was large, and the relative wind speed was fast; thus, the fuel consumption was relatively high, as indicated by the increase in the red indicator. Due to the large area of the hull, the sway was increased during the voyage. Once the voyage was increased, the resistance was also large and high fuel consumption was possible.



(a) Statistics of wind speed and wind direction (b) Frequency between wind direction and wind speed  
 Fig. 3 Distribution of statistics and frequency for wind speed vs. wind direction, respectively

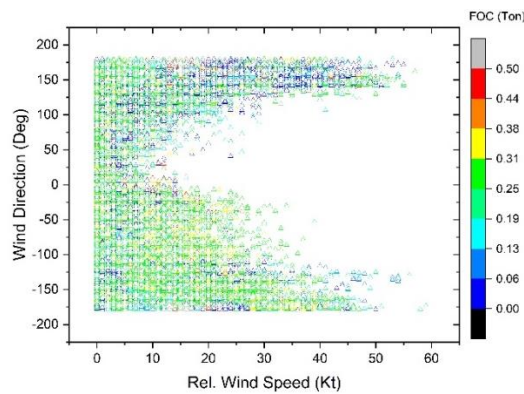


Fig. 4 Comparison of relative wind direction (degree) and speed vs. main engine fuel consumption

Fig. 5 illustrates the relationships between the speed through water (STW) as well as the SOG and the main engine (ME) power, main shaft speed, and the relative wind speed. The upper left (a) and upper right (b) figures show the relationships between SOG and ME power and main shaft speed, respectively. The lower left (c) and right diagrams (d) show the relationships between the STW and the ME power and main shaft speed, respectively. The color bar on the right of the figure indicates the relative wind speed. The stronger the red, the weaker the blue. As a result, the ship's speed and wind speed increase and vice versa.

Fig. 6 presents cross views of a combined statistical distribution of the ME power and STW frequencies. The frequency statistics of the ME power at 0~38,000 KW is shown in the upper Fig. 6(a). The frequency of the ME was up to 46,000 KW, which is used for low-speed operations, and the captain relied on the power; the other different power times were between 1 and 30; this range cannot be clearly displayed due to the limitation of the unit scale in the chart. In the lower Fig. 6(a), the occurrences of the STW is shown. The figure shows that the ship's speed had the second-highest frequency when it was at 0 knots, but the highest frequency was around 18 knots, which also means that the ship's speed was economical. At the Fig. 6(b), the ME power is integrated with the STW. As a result, the blue color indicates the STW and the red indicates the ME power. On the other hand, The SOG depends on the ocean currents and weather at sea and indirectly affects the ME output power.

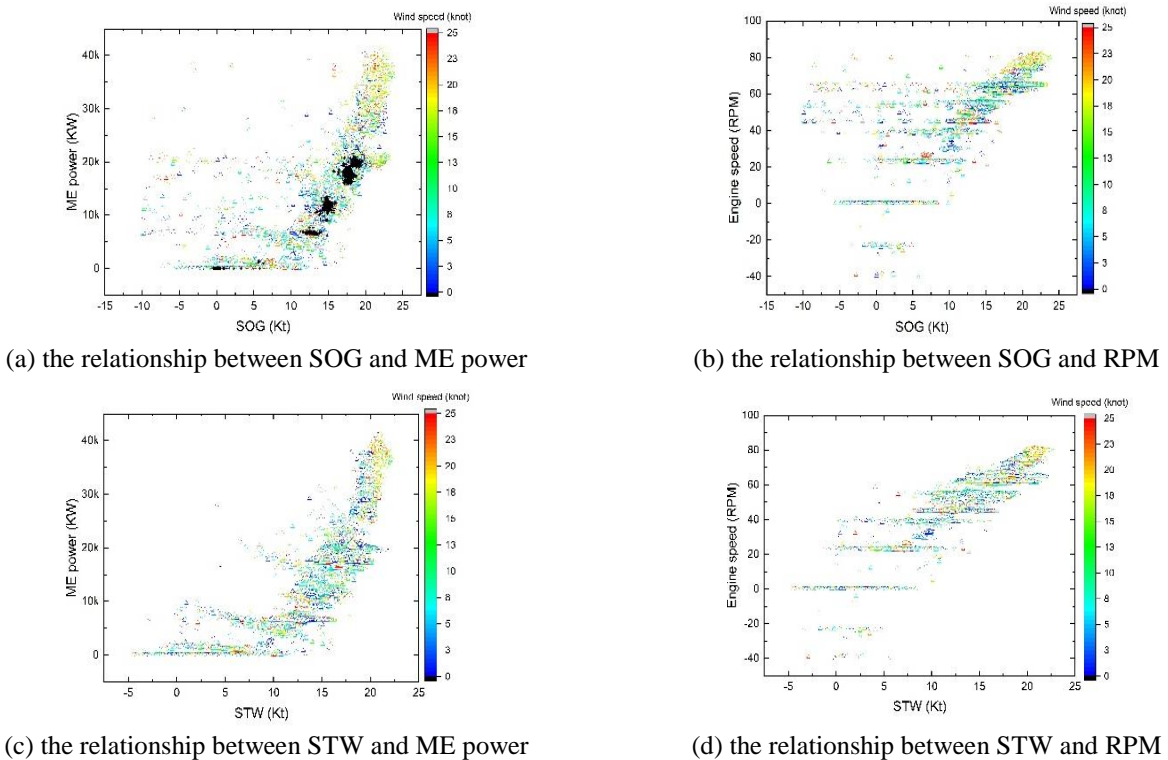
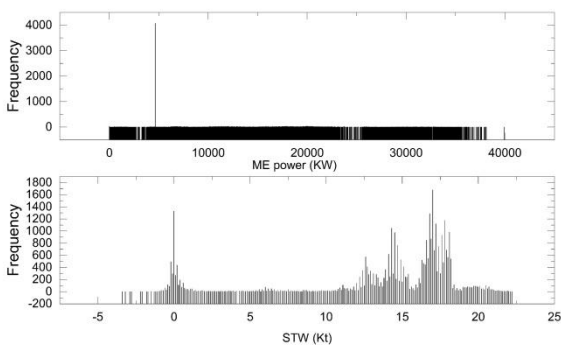
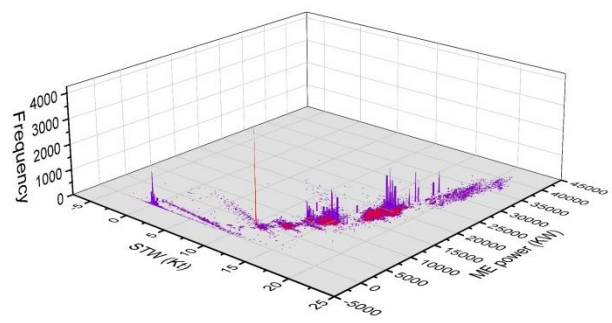


Fig. 5 Distribution of speed, power profile and wind speed



(a) Statistics of ME power and STW



(b) Frequency between STW and ME power

Fig. 6 Distribution of statistics and frequency for ME power vs. STW, respectively

Fig. 7 shows an exponential function or a polynomial distribution for the relationship between the STW and ME power, where the right color bar is red at maximum fuel consumption and blue at minimum fuel consumption. When the STW on the abscissa is higher than 20 knots, the fuel consumption increases in the red or even gray area. Both the horizontal and vertical coordinates are exponential functions. Among them, the horizontal stripe appearing on the surface indicates that the navigation at this stage was affected by ocean currents. In addition, radio noise sometimes interfered with the data collection on the ship. Because the big data hardware was installed in the electrical room, it might have been affected by a heat wave, humidity, and temperature; however, these data can be ignored. Fig. 8 illustrates the relationship between the STW and ME power. The bar on the right shows the SOG. The red indicates the ahead speed of the ship. The higher the speed, the faster the ship. The SOG is the actual sailing distance, which is affected by the influence of tidal current, wave, and climate on the water speed. Sometimes, the SOG was higher than the STW, but the ship's speed was reduced when it was affected by the resistance of the current. For example, when the SOG was in the 17~24 knots, the STW was about 20 knots, which means that the forward or reverse flow or the wind resistance affected the speed of the ship.

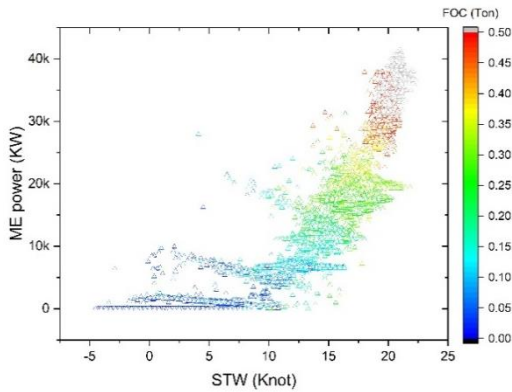


Fig. 7 A profile illustration involving STW, ME power, and fuel consumption

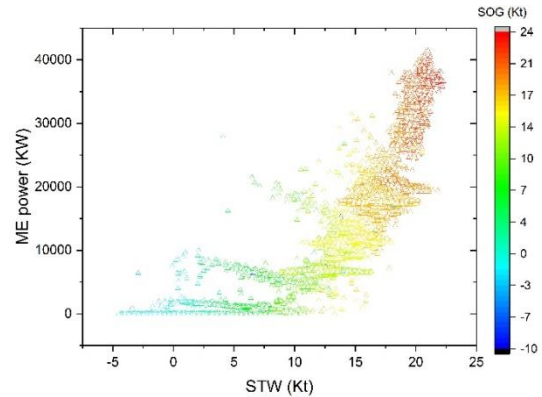


Fig. 8 A distribution of STW and ME power vs. SOG

Fig. 9 illustrates the relationship between the engine speed, ME power, and fuel consumption. The right side is a color bar indicating fuel consumption, where red is the highest fuel quantity, which is decremented in turn, and blue is the minimum fuel quantity; the faster the shaft speed, the more the fuel consumption. The figure shows that fuel consumption conditions were normal when the main shaft speed was about 40~60 revolutions per minute (rpm). Once the speed exceeded 80 rpm, the fuel consumption was very high, and it falls in the red area or even the gray stage in the figure. From the experiment, it can be concluded that the ship operation was usually under 75% ME power and energy was saved. In addition, the maneuvering system was controlled by a governor, which could stabilize the speed of the main shaft. When the ship navigation was affected by the external climate and ocean current, the system sent a feedback signal to adjust the fuel injection to maintain a stable speed of the main shaft. At this moment, the ME power will change accordingly. Therefore, the profile of ME power in Fig. 9 is a fluctuation against environmental variation.

Fig. 10 illustrates the analysis of STW and ME power versus the speed of the main shaft, where STW is dependent on the power level of the ME. The color pattern on the right represents the main shaft speed. When the STW was high, the ME ran at high power, and the fuel consumption increased accordingly.

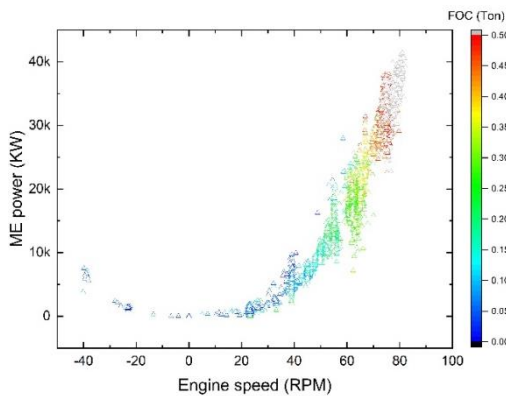


Fig. 9 Distribution of engine speed and ME power vs. FOC

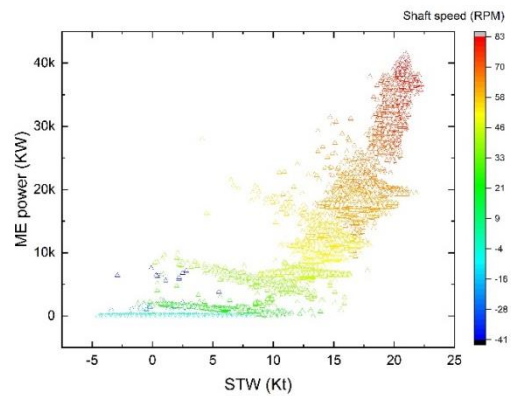
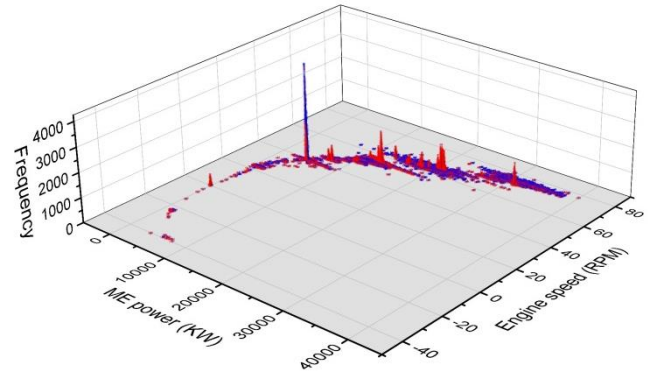
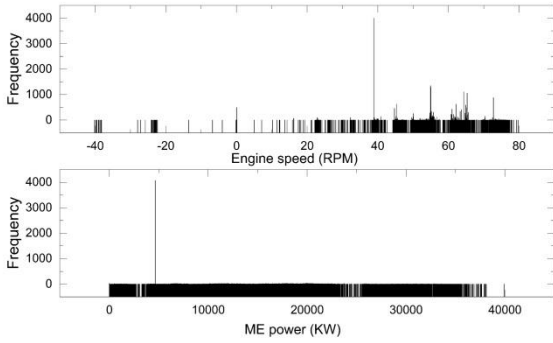


Fig. 10 Profile of STW, ME power, and shaft speed (rpm)

Fig. 11 presents the cross views of a combined statistical distribution of the engine speed and ME power frequencies. The upper Fig. 11(a) depicts the frequency statistics of the engine speed, of which 40 rpm had the highest frequency, about 4,000 times for this ship, due to the needs for special sea detail and along the coastline. Moreover, the engine speed can reduce the emission pollution which is used the speed of the same type of ship. Second, the speeds were 55, 65, 70, and 75 rpm. Furthermore, the lower Fig. 11(a) shows the peak frequency, which also conforms to a power of 40 rpm. The Fig. 11(b) indicates the frequency statistics of the two parameters, in which the blue color represents the ME power and the red color represents the main shaft speed (rpm). Both frequencies are integrated into the vertical axis, and the highest peak can be observed as 40 rpm.



(a) Statistics of engine speed (RPM) and ME power

(b) Frequency between ME power and engine speed (RPM)

Fig. 11 Distribution of statistics and frequency for engine speed vs. ME power, respectively

Fig. 12 presents the relationship between the average draft, trim, and fuel consumption. The right color bar indicates the fuel consumption measured in metric tons. It can be seen that the draft was below 10.5 m. The fuel consumption was still high even if the trim by the stern was between 0 and 0.5 m. The average draft and the load are significant parameters that affect fuel consumption. In addition, improper control of the trim will also increase the ship’s resistance. The trim by the stern indicates that the bow is lifted, and the trim by the head indicates that the bow is sinking. The data show that the bow was always sinking in the containership. From the experiment results, it is recommended that the ship should utilize the ballast water to deliver to the stern section that increases the draft of the aft. Fig. 13 illustrates the relationship between the average draft, STW, and ME power. The coordinate is the STW and the ordinate is the ME power. The right color bar represents the draft; red indicates the draft at deep depth, while blue indicates the draft at shallow depth. The results show that the STW is related to the ME power, and the relationship features a curve phenomenon. By statistics, the 12-meter draft was at a speed of over 18 knots.

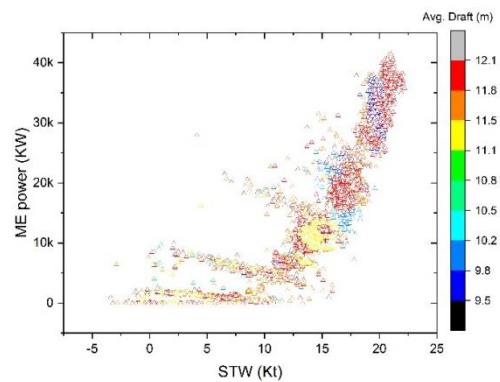
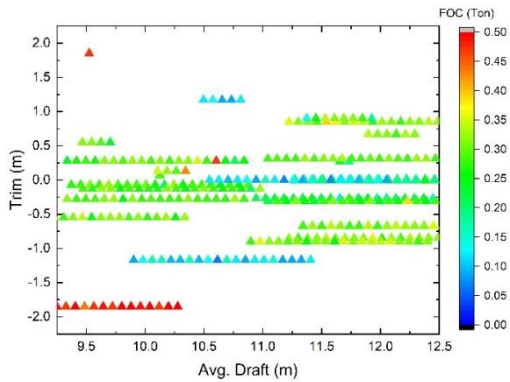


Fig. 12 Profile of average draft and trim with respect to ME fuel consumption

Fig. 13 Profile of STW and ME power with respect to average draft

Fig. 14 presents the cross views of a combined statistical distribution of the average draft and trim frequencies. The frequency statistics of the average draft is depicted in the upper Fig. 14(a). The plot shows that the draft depth of 12 m was the most used in the navigation, followed by the adjacency of 11.8 m, and then the depth of about 10 m. The lower Fig. 14 (a) graph shows the statistical result of the trim. When the trim is 0 m, the frequency is about 8000 times, and the sequence order is -0.3, -1, and -1.2 m, which can show the tendency at the trim of the ship. As a result, the trim by the head occurred more times than the trim by the stern. The Fig. 14(b) shows the distribution of the average draft and trim; blue represents trim and yellow represents the average draft.

Fig. 15 displays the relationships between the trim and the STW and ME power. The result is similar to the previous figure and features an exponential function relationship. The right of the figure shows the height of the trim; where the red color represents the trim by the stern, and the blue represents the trim by the head. As a result, the statistics show that the trim fell to

near 0 m and the frequency of trim by the head was much more than trim by the stern. In addition, Fig. 16 shows the distribution of the calculated EEOI statistic.

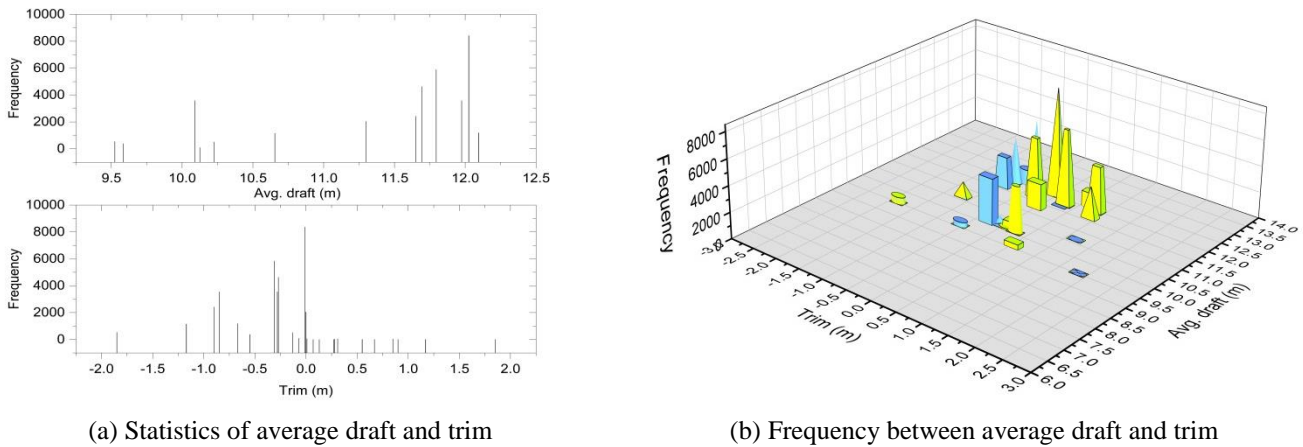


Fig. 14 Distribution of statistics and frequency for average draft vs. trim, respectively

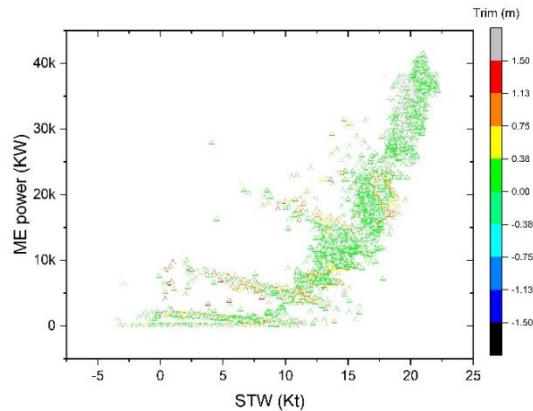


Fig. 15 Profile of STW and ME power with respect to trim

Fig. 16 shows the relationship between the trim, avg. draft, FOC, sailing distance, cargo mass, and EEOI. The figure is divided into five operational windows: A, B, C, D, and E. The trim is the difference between the aft draft and the fore draft, and the avg. the draft is an average of the aft draft and fore draft. FOC means fuel consumption. The sailing distance is the distance traveled in nautical miles. Moreover, SOG is the real speed displayed on the GPS, which is the vessel speed relative to the earth surface. Cargo mass expresses the carrier capability of the ship. The EEOI represents a metric unit of CO<sub>2</sub> per nautical mile and cargo mass, and it is an indication of CO<sub>2</sub> emission quantity. As a result, the trim is dependent on the height difference between the fore draft and aft draft, which is one of the major factors that affect the energy-saving strategy. The trim was approximately at 0 m to 0.8 m, an acceptable range considering the various sailing conditions. Despite the minor effect of the trim on the EEOI in the experiment, the avg. the draft was a major factor that affected the EEOI. Consequently, the operational window of A indicates low draft around 10 m but high emission (EEOI). However, the average drafts around 12 m shown in windows B, C, D, and E correspond to a lower CO<sub>2</sub> emission than that of window A. Thus, the energy saving phenomenon illustrates a quite remarkable and more saving of fuel oil at an average draft of 12 m. On the other hand, cargo mass is a function of draft, and both parameters interact with each other. Furthermore, the ballast water is an alternative method to adjust the suitable draft depth. Window A indicates light cargo mass, but fuel consumption is worsened and the EEOI increases. Windows B, C, D, and E illustrate a heavy cargo mass, but low fuel consumption and low EEOI, which is in the range of  $1\sim3 \times 10^{-5}$ . Consequently, the cargo mass significantly affected energy efficiency. The EEOI variation for over six months was successfully investigated by statistical analysis of the sailing condition.

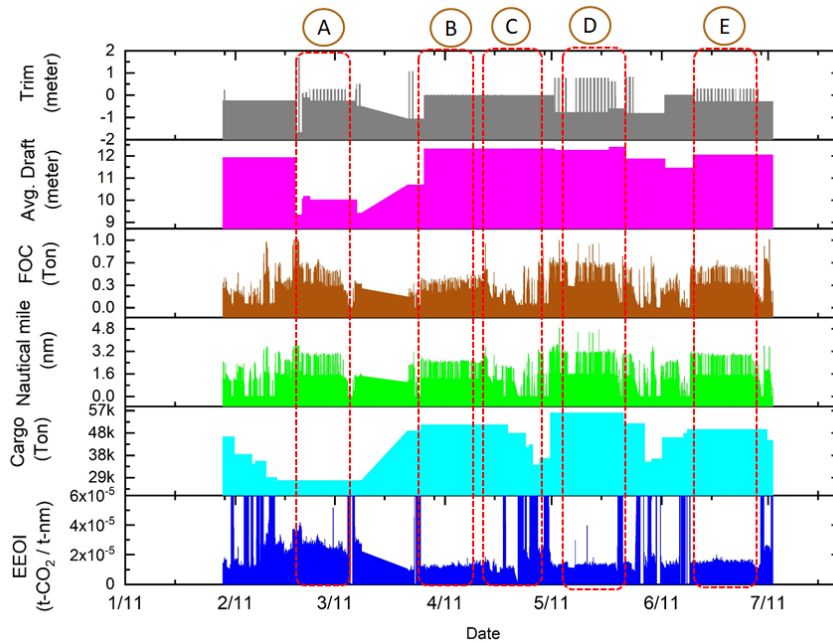


Fig. 16 EEOI calculation for various cargo masses, distances, FOCs, avg. drafts, and trims

Table 2 presents the quantitative intensity of emission index for each window of Fig. 16 in the order of the EEOI. Window B corresponds to the strategy with the least EEOI. Window D also features a low EEOI but has the highest cargo mass than that of the condition if the captain chooses the option. Window A corresponds to the worst energy-saving strategy; thus, the captain must avoid this operational condition.

Table 2 Quantitative index for each window according to the EEOI

Window	Date duration	EEOI × 10 <sup>-5</sup>	Mass (ton)	Distance (nm)	FOC (Mt)	Avg. draft (m)	Trim (m)
B	4/3~4/22	1.50	50,803	1.19	0.19	11.86	-0.15
D	5/21~6/4	2.46	54,980	1.43	0.27	11.95	-0.79
E	6/9~7/8	2.17	47,239	1.21	0.22	11.65	-0.29
C	5/3~5/15	2.72	45,337	1.21	0.25	12.01	-0.23
A	2/28~3/18	5.01	27,254	1.38	0.28	10.06	-0.43

Table 3 A quantitative result showing the differences and values from max. to min

Windows	EEOI	Mass	Distance	FOC
B	10.8%	22.5%	18.6%	15.8%
D	17.7%	24.4%	22.2%	22.6%
E	15.7%	20.9%	18.9%	18.2%
C	19.6%	20.1%	18.9%	20.3%
A	36.1%	12.1%	21.4%	23.1%
Differ	25.3%	12.3%	3.6%	7.3%
Value	3.51*10 <sup>-5</sup> (t-CO <sub>2</sub> /t-nm)	27,726 (ton)	0.23 (nm)	0.09 (ton)

Table 3 summarizes the analysis results of the percentage difference between the maximum and minimum energy efficiency parameters during different voyages. Statistics for interval windows A, B, C, D, and E are presented. The EEOI difference is the amount of CO<sub>2</sub> emissions, and the EEOI value of each interval is divided by the amount of each interval; for example, for the B interval, the formula is (EEOI value of B)/(EEOI value of A + B + C + D + E). The value for each interval is taken, and then the maximum value is subtracted from the minimum value to obtain the difference in amount.

The results show that EEOI could be reduced to 25.3%, which corresponds to a CO<sub>2</sub> emission reduction of 3.5 × 10<sup>-5</sup>. In the same way, the load capacity was increased by 12.3% or 27,726 tons; the travel distance was increased by 3.6% or 0.23 nautical miles, and fuel consumption was saved by 7.3% or 0.09 tons. Therefore, adjusting the load and draft can reduce the CO<sub>2</sub> emissions and fuel consumption of the ship and provide positive guidance to ship decision makers.

A forward-looking energy efficiency strategy for smart shipping through a big data analysis device is developing in this work. For various conditions of the vessel, the sailing mode can be selected based on an evaluation of energy saving and emission control. The variation of EEOI with the trim, avg. draft, FOC, distance, cargo mass indicates a clear relationship. For this type of container ship, a draft between 11.5 m and 12 m is suitably deep to reduce fuel consumption. This energy-saving strategy can significantly save fuel oil and reduce the CO<sub>2</sub> emission quantity, as opposed to the traditional concept in the shipping industry. Furthermore, both cargo mass and ballast technique always interact with the draft depth of the ship. A constructive model using IoT technology and an energy efficiency management strategy presents an accurate big data basis to guide decision making on the vessel. The results showed that the EEOI (the CO<sub>2</sub> emission) was reduced by 25.3%, the ship could carry an additional cargo mass of 12.3%, the travel distance (nautical mile) was increased by 3.6%, and then fuel oil was saved by 7.3%. Thus, the maritime industry can improve the energy saving and engine efficiency of ships using the EEOI-based model.

## Acknowledgement

This project is financially supported by the program “Data Analytics for Smart Shipping and Marine Energy Management” of the Ministry of Science and Technology, Taiwan, R.O.C. under grant no. MOST 107-2218-E-006 -042. Moreover, the authors thank Enago ([www.enago.tw](http://www.enago.tw)) for providing professional English review services.

## Conflicts of Interest

The authors declare no conflict of interest.

## References

- [1] M. D. A. Al-Falahi, K. S. Nimma, S. D. G. Jayasinghe, H. Enshaei, and J. M. Guerrero, “Power management optimization of hybrid power systems in electric ferries,” *Energy Conversion and Management*, vol. 172, pp. 50-66, September 2018.
- [2] L. P. Perera and B. Mo, “Emission control based energy efficiency measures in ship operations,” *Applied Ocean Research*, vol. 60, pp. 29-46, October 2016.
- [3] M. Tichavska, B. Tovar, D. Gritsenko, L. Johansson, and J. P. Jalkanen, “Air emissions from ships in port: Does regulation make a difference?” *Transport Policy*, vol. 75, pp. 128-140, March 2019.
- [4] R. D. Prasad and A. Raturi, “Fuel demand and emissions for maritime sector in Fiji: Current status and low-carbon strategies,” *Marine Policy*, vol. 102, pp. 40-50, April 2019.
- [5] K. Lehtoranta, P. Aakko-Saksa, T. Murtonen, H. Vesala, L. Ntziachristos, T. Ronkko, et al., “Particulate mass and nonvolatile particle number emissions from marine engines using low-sulfur fuels, natural gas, or scrubbers,” *Environmental Science & Technology*, vol. 53, pp. 3315-3322, March 2019.
- [6] Y. H. Hou, “Hull form uncertainty optimization design for minimum EEOI with influence of different speed perturbation types,” *Ocean Engineering*, vol. 140, pp. 66-72, August 2017.
- [7] T. A. Tran, “A research on the energy efficiency operational indicator EEOI calculation tool on M/V NSU JUSTICE of VINIC transportation company, Vietnam,” *Journal of Ocean Engineering and Science*, vol. 2, pp. 55-60, March 2017.
- [8] *Shipbuilding — Principal ship dimensions — Terminology and definitions for computer applications*, ISO 7462, 1985.
- [9] H. J. Shaw, W. G. Teng, and F. M. Tzu, “A study on energy efficiency management for smart ships,” 3rd International Naval Architecture and Maritime Symposium, Proceedings, Yıldız Technical University, Istanbul, Turkey, pp. 657-668, 2018.
- [10] P. Kaluza, A. Kolzsch, M. T. Gastner, and B. Blasius, “The complex network of global cargo ship movements,” *Journal of the Royal Society Interface*, vol. 7, pp. 1093-1103, July 2010.
- [11] M. Svindland, “The environmental effects of emission control area regulations on short sea shipping in Northern Europe: the case of container feeder vessels,” *Transportation Research Part D-Transport and Environment*, vol. 61, pp. 423-430, June 2018.
- [12] L. Zhen, M. Li, Z. Hu, W. Y. Lv, and X. Zhao, “The effects of emission control area regulations on cruise shipping,” *Transportation Research Part D-Transport and Environment*, vol. 62, pp. 47-63, July 2018.

- [13] M. Jurjevic, N. Koboevic, and M. Bosnjakovic, "Modelling the stages of turbocharger dynamic reliability by application of exploitation experience," *Tehnicki Vjesnik-Technical Gazette*, vol. 25, pp. 792-797, June 2018.
- [14] Z. Koboevic, D. Bebic, and Z. Kurtela, "New approach to monitoring hull condition of ships as objective for selecting optimal docking period," *Ships and Offshore Structures*, vol. 14, pp. 95-103, January 2019.
- [15] "IMO Train the Trainer (TTT) Course on Energy Efficient Ship Operation, Module 2–Ship Energy Efficiency Regulations and Related Guidelines," Printed and published by the International Maritime Organization, vol. 2, p. 42, 2016.



Copyright© by the authors. Licensee TAETI, Taiwan. This article is an open access article distributed under the terms and conditions of the Creative Commons Attribution (CC BY-NC) license (<https://creativecommons.org/licenses/by-nc/4.0/>).